Journal of Atmospheric and Solar–Terrestrial Physics 211 (2020) 105462

Contents lists available at ScienceDirect

Journal of Atmospheric and Solar-Terrestrial Physics

journal homepage: www.elsevier.com/locate/jastp

Research Paper

Observational evidence of equatorial ionospheric response to severe cyclonic storms 'AILA' and 'WARD' observed over the North Indian Ocean

G.J. Bhagavathiammal, Dr., Assistant Professor [a,*], Manohar Lal [b], K. Emperumal [c]

[a] Anna University, Department of Medical Physics, CEG Campus, Sardar Patel Road, Guindy, Chennai, 600025, Tamil Nadu, India
[b] K.S. Krishnan Geomagnetic Research Laboratory, Indian Institute of Geomagnetism, Allahabad, Uttar Pradesh, 211019, India
[c] Equatorial Geophysical Research Laboratory, Indian Institute of Geomagnetism, Tirunelveli, 627011, Tamil Nadu, India

ARTICLE INFO

Keywords:
Tropical cyclone
Ionosphere
Gravity waves
Convection

ABSTRACT

This work addresses the vertical atmosphere –ionosphere coupling through two cyclonic events AILA (23–26 May 2009) and 'WARD' (10–16 December 2009) observed over the North Indian Ocean. Combined ground Digisonde Tirunelveli (8.7^{o}N, 77.8^{o}E) observation, ECMWF reanalysis, and NOAA Outgoing Longwave Radiation data used to reveal the connection between atmosphere –ionosphere system. At the time of tropical cyclone, we observed a decrease in surface pressure and an increase of sustained oceanic winds. Thereby increases the tropical convection observed from the lowered OLR (Outgoing Longwave Radiation). The existence of Gravity wave oscillations of period ~4 h at the stratosphere and ionosphere regions indicate the propagation of low-frequency GWs (Gravity Waves) from the lower atmosphere. Weak eastward stratospheric winds observed at the time of onset of the cyclonic storm in both AILA and WARD events. The Ionospheric parameter foF2 and h'F2 show strong modulation at the time of cyclones AILA and WARD.

1. Introduction

The ionospheric response to tropospheric meteorological events has been studied for more than 40 years. But the effect of meteorological phenomena on the ionosphere is still a complicated morphology. Tropical Cyclones are deep storms having extreme winds with organized convective systems. The different stages of cyclone growth are low pressure, deep depression, cyclonic storm, and severe cyclonic storm, etc. The progress of cyclone intensification starts from low pressure to severe cyclonic storm (Roy and Kovordanyi, 2018). The relation between meteorological phenomena and ionosphere was studied many decades (Gherzi, 1950; Bauer, 1957, 1958; Arendt and Frisby, 1968; Shresta, 1971a, b; Kersley and Rees, 1982; Goldberg, 1991; Chen, 1992, Yi and Chen, 1993, Manzano et al., 1998, Mikhailov et al., 2005; Vanina-Dart et al., 2007a, 2007b, 2008; Bauer, 1957, 1958; Shen, 1982, etc.) Summary of the published results on the possible effects of the tropical cyclones are.

1. The descent of ionosphere reflection height with the advance of the direction and movement of a hurricane.
2. Increase of critical frequencies with the hurricane approach
3. The variation of sporadic layer parameter with the passage of fronts.
4. Launch of planetary and gravity waves by weather fronts and other sources in the troposphere and stratosphere, capable of propagating into the ionospheric F2 region where their energy dissipated through the act of viscosity.
5. Variability in equatorial ionization by Quasi-Biennial Oscillation (QBO).
6. Lighting effects at the lower ionosphere.
7. Generation and propagation of medium-scale gravity waves from tropospheric sources into the ionosphere.

The ionosphere is an electrified layer. The forcing from above and below regions of the atmosphere profoundly modifies the structure and dynamics of the ionosphere. The effect of meteorological processes on the ionosphere through the upward propagating atmospheric waves ranging from small scale acoustic waves with periods ranging from minutes to large scale planetary waves was significant (Lastovicka, 2006; Knížová et al., 2015). In recent decades, the effect of atmospheric waves on the ionospheric F layer was reported by many authors (Forbes and Leveroni, 1992; Pancheva et al., 1994; Lastovicka and Sauli, 1999; Afraimovich et al., 2000; Boska and Sauli, 2001; Altadill et al., 2004; Radicella et al., 2009; Knížová et al., 2015; Cang et al., 2015).

Hung and Kuo (1978) reported the appearance of gravity waves of

* Corresponding author. Department of Medical Physics, Anna University, CEG Campus, Sardar Patel Road, Guindy, Chennai- 600025, India.
E-mail address: bhagavathy.gj@annauniv.edu (G.J. Bhagavathiammal).

https://doi.org/10.1016/j.jastp.2020.105462
Received 14 November 2019; Received in revised form 19 September 2020; Accepted 21 September 2020
Available online 8 October 2020
1364-6826/

periods of 15–30 and 27–30 min in the ionosphere F region during an extreme tornado outbreak. The study by Perevalova and Polekh (2009) reveals the mid-latitude upper atmospheric response to tropical cyclones. They found the propagation of gravity waves of periods 1.5–6 h as traveling ionospheric disturbances (TIDs). Polyakova and Perevalova (2013) have shown an increase in Total Electron Content (TEC) with internal wave signatures in the ionosphere at the time of tropical cyclone. Their study depicts ionospheric response not only depends on the intensity of cyclone but also the background condition that affects the wave propagation. Lin (2012) detected the spatial TEC anomaly distribution associated with Typhoon Nakri (May 29, 2008). Sindelarova et al. (2009) revealed the occurrence of acoustic gravity waves of period 2–30 min in the ionosphere during tropospheric convective storms over the Western and Central Parts of the Czech Republic.

Many researchers contributed to the typhoons-ionosphere coupling (Kazimirovsky, 2002; Sun et al., 2007; Xu et al., 2008; Mao et al., 2009; Liu et al., 2010). Bishop and Straus (2006) examined ionospheric variation during MATSA typhoon (01–10 August 2005) passed over China using GPS Occultation. They observed significant TEC scintillation within 1200 km of a storm center. Mao et al. (2009) found an unusual change in foF2 and TEC at the time of arrival of the typhoon.

In **2011**, (Polyakova and Perevalova, 2011) examined the ionospheric response to tropical cyclones KATRINA, RITA, and WILWA using GPS receiver and NCEP/NCAR Reanalysis data. For the first time in India, Guha et al. (2016) studied the equatorial ionospheric response to tropical cyclone MAHASEN (2013) and HUDHUD (2014) using GPS Observation. Their study suggests that the combined effect of Tropical cyclone-inspired gravity waves as one of the causes for the observed ionospheric anomaly.

The present work investigates the equatorial ionospheric response to severe cyclonic storms 'AILA' (23–26 May 2009), and 'WARD' (10–16 December 2009) observed over the North Indian ocean. In this investigation, we have utilized the observational cyclone data from Indian Meteorological Department, New Delhi, Digisonde ground observation located at dip-equatorial station, Tirunelveli (8.7^{o}N, 77.8^{o}E), ECMWF ERA-Interim Reanalysis and NOAA -Interpolated Outgoing Longwave Radiation (OLR) data.

2. Data used

2.1. Cyclone data from IMD

The cyclone track and data obtained from the India Meteorological Department, New Delhi, archived at http://www.rsmcnewdelhi.imd.gov.in/index.php?lang=en.

2.2. Dst and Kp indices

The region ionosphere is responsive to both upper and lower atmospheric forcing. The condition of solar and geomagnetic activities modulates the electrified ionospheric layer. Hence, the geomagnetic state needs to be confirmed to visualize the lower atmospheric response in the ionosphere. The indices Dst and Kp signifies the global geomagnetic activities at the time of cyclone events AILA and WARD (Pulinets et al., 2003).

The indices Dst and 3-Hour Kp index have obtained from the World Data Centre of Geomagnetism, Kyoto http://wdc.kugi.kyoto-u.ac.jp/.

2.3. Outgoing Longwave Radiation (OLR) data

Interpolated daily Outgoing Longwave Radiation (OLR) data is obtained from the Climate Diagnostic Center (CDC) of the National Oceanic and Atmospheric Administration (NOAA) Satellite. The OLR data taken were gridded into 2.5° latitude × 2.5° longitude grid, used as a proxy for deep tropical convection (Hendon and Woodberry, 1993). A complete description of the (interpolated) OLR dataset was given by Liebmann and Smith (1996). The data presented here are smoothed using the 5-day running average.

2.4. Digisonde observation at tirunelveli

The routine measurements of the ionosphere have taken using Digital Ionosonde.

(Canadian Advanced Digital Ionosonde) operated at the dip-equatorial station, Tirunelveli (8.7^{o}N, 77.8^{o}E), India. The standard ionograms have recorded at a resolution of 15 min interval. However, occasional ionograms of 5/10 min resolution are also available. The present study utilizes ionospheric parameters foF2 (critical frequency of F2 layer) and h'F2 ((lowest virtual height of the F2 trace)) for the two cyclone events AILA (23–26, May 2009) and WARD (10–16 December 2009). The sampling rate of the ionospheric data used in this study has 10 min interval (600 s). Ionosonde helps to detect the ionospheric plasma as a function of height. The ionosonde transmits HF radio waves (typically 1–20 MHz) vertically and records the time-of-flight of "echoes" reflected from the various ionized layers. Receiver antennas co-located with the transmitter detect the return echoes from the ionosphere. The day time foF2 and h'F2 values have taken into account for this study. The day time foF2 and h'F2 profiles show three small data gaps (10-11LT, 11.5–12.5 LT and 14.6–15.1LT) on May 26, 2009 and single data gap between 10 and 12 LT on December 11, 2009. Continuous day time records of foF2 and h'F2 are noted on other days in both the events, from 23 to May 25, 2009 and 10, 12–16 December 2009.

2.5. ECMWF ERA-Interim Reanalysis

ECMWF ERA-Interim Reanalysis helps to reveal the dynamical aspects of the stratosphere (Dee et al., 2011). This study utilizes wind components having spatial coverage 1.5° latitude and 1.5° longitude grid extends the pressure levels from 1000 to 1 hPa corresponds to ~0.1 and ~50 km (37 levels). The wind components are achieved from ECMWF website http://data-portal.ecmwf.int/data/d/interim_daily/.

2.6. Life cycle of AILA and WARD cyclone

2.6.1. Severe cyclonic storm "AILA" (23–May 26, 2009)

AILA is a severe cyclonic storm disturbance formed during the premonsoon season over the Bay of Bengal (BOB) (23–May 26, 2009). On May 22, 2009, a low-pressure area formed over the east-central BOB and neighbourhood. On May 23, 2009, this well-marked low pressure concentrated into a Depression and lay centered at 0600 UTC near 16.5^{o}N/88.0^{o}E. It is intensified into a deep depression on May 24, 2009 near 18.0^{o}N/88.5^{o}E and into becoming a Cyclonic Strom "AILA" near 18.5°N/88.5°E. Further, it intensified into a Severe Cyclonic Storm on May 25, 2009 near 21.5°N/88.0°E. It became weakened into Cyclonic storm and Deep Depression on May 26, 2009 (India Meteorological Department Annual Report, 2009; https://metnet.imd.gov.in/imdnews/ar2009.pdf).

2.6.2. Severe cyclonic storm "WARD" (10–16 December 2009)

A low-pressure area was formed over the southwest and adjoining the southeast Bay of Bengal on December 8, 2009. It became well marked and concentrated into a Depression over southwest and adjoining southeast Bay of Bengal and neighbourhood near 6.5°N/85.0°E on December 10, 2009. Moving towards north westwards, it became intensified into Deep Depression on December 11, 2009 (centered near 7.0°N/84.5°E). Subsequently, it moved northwards and strengthened into Cyclonic Storm 'WARD' near 8.5°N/84.5°E on December 11, 2009. After that, it moved westwards near 10.0° N/83.5° E on December 12, 2009. Drifting southwards, it weakened into a Deep Depression and lay centered near 9.5°N/83.5°E. Moving westwards, it lay over the southwest Bay of Bengal centered near 9.5°N/83.0°E on December 13, 2009 and further drifted southwards, close to Trincomali, Sri Lanka on December 14, 2009. It crossed north Sri Lanka coast near Trincomali and weakened into a depression and lay centered over the north of Sri Lanka, near 8.5°N/81.0°E on 14 December, further weakened into a well-marked low-pressure area over Sri Lanka and neighbourhood on December 15, 2009. It laid and less marked over Gulf of Mannar and adjoining North Sri Lanka and Coastal Tamil Nadu on December 16, 2009. The observed lowest Central Pressure was 996 mb, and the maximum wind speed observed was 45 knots. Vigorous Northeast monsoon followed on December 16, 2009. (India Meteorological Department Annual Report, 2009; https://metnet.imd.gov.in/imdnews/ar2009.pdf).

3. Results and discussion

Fig. 1 depicts the cyclone tracks of events AILA and WARD, and the location of Digisonde observatory, Tirunelveli (8.7°N, 77.8°E). The observational site Tirunelveli (8.7°N, 77.8°E) has marked on the map with a yellow circle. The Cyclone tracks AILA and WARD are labeled in Red and Black Color, respectively.

3.1. Temporal variation of foF2 and h'F2

Fig. 2 describes the temporal variation of foF2 and h'F2 (0–24 LT hours) during the cyclone AILA and WARD. The left panel of Fig. 2 shows the temporal variation of foF2 (bottom) and h'F2 (top) at the time of cyclone AILA. The peak of h'F2 shows some significant change of rising from 435 km to 585 km at the time of AILA cyclone transformation from deep depression into a severe cyclonic storm on May 25, 2009. This sustained h'F2 increase continues on May 26, 2009, At the same time, the peak of foF2 shows a substantial decrease of about ~0.85 MHz on May 26, 2009 at the time of cyclone transformation from cyclonic storm into a deep depression. The right panel of Fig. 2 shows the temporal variation of foF2 (bottom) and h'F2 (top) at the time of cyclone WARD. We found the peak of h'F2 increases by 40 km and foF2 suppresses by 1 MHz from depression into a cyclonic storm stage on December 11, 2009. Followed by, a sudden drop (~90 km) in the peak of h'F2 happens on December 13, 2009 at the time of deep depression. Whereas, the foF2 shows a stepwise increase from 11 to December 16, 2009. The reason for the appearance of the opposite trend of either increase or decrease of ionospheric foF2 and h'F2 depends on (i) the position of tropical cyclone (TC) from the point of view of its landing (Tian et al., 2009) (ii) the distance from the source location of cyclone and observation site and (iii) delay of the measurement moment relative to the beginning of TC action (L. B. Vanina Dart et al. (2011)).

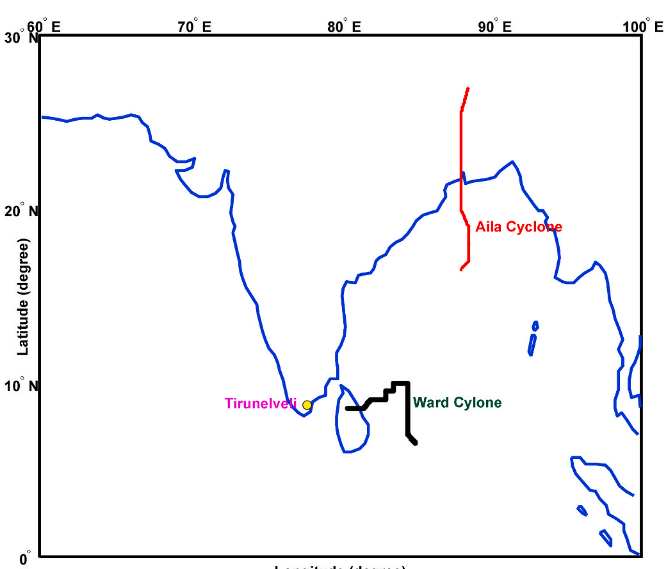

Fig. 1. Track of Cyclones AILA and WARD, and the location of Ionosonde observatory, Tirunelveli (8.7°N, 77.8°E).

Fig. 2a represents the local time variation of foF2 and h'F2 (9–17 LT hours) during the cyclones AILA (top) and WARD (bottom). As we can see from Fig. 2a, the foF2 minimizes around 10–11 LT hours and maximizes about 15–16 LT hours. The maximum value of h'F2 recorded around 10–11 LT hours when the foF2 minimum. The profile of foF2 and h'F2 in both the cyclones AILA and WARD reveals an opposite trend. As we can infer from AILA cyclone, the significant enhanced (suppressed) of foF2 (h'F2) noticed at the start of depression on May 23, 2009. The reverse of the same (low foF2 and high h'F2) was found on May 26, 2009 at the time of the weakening of cyclonic storm into deep depression. On May 24, 2009, the cyclone intensification as deep depression suppresses both foF2 and h'F2, But at the time of cyclonic storm (May 25, 2009) stage, the foF2 and h'F2 increases strongly.

The bottom left (right) panel describes the foF2 (h'F2) variation at the time of the WARD cyclone. On December 11, 2009, we found a suppressed (enhanced) foF2 (h'F2) at the transition from depression into cyclonic storm. The modulated pattern of foF2 and h'F2 found on December 13, 2009 at the time of weakening into deep depression. The modulating foF2 and h'F2 variations are found in the case WARD cyclone, which has not seen in the other one. As we infer from Fig. 2(a), the opposite trend of suppressed foF2 and enhanced h'F2 in WARD differing from AILA might due to the (i) the position of the TC is different from the point of view of its landing. (ii) The distance of separation from cyclone location to the observation site is ~830 Km to ~632 Km (1447 Km to 2324 Km) in the case of WARD (AILA) and (iii) delay of the measurement moment relative to the beginning of TC action.

3.2. Oceanic surface wind, central pressure, and OLR variation

Fig. 3 represents the temporal variation (23–26 May 2009) of observed oceanic surface wind and estimated central pressure (bottom) concerning the latitude time variation of OLR averaged over 80-90°E during the cyclones AILA and WARD (top). The left panel describes the latitude time variation of OLR averaged over 80-90°E related to surface wind and estimated central pressure during the cyclone AILA. The oceanic surface wind starts increases from May 24, 2009 and maximizes on mid-day of May 25, 2009. At the same time, central pressure starts to decline from May 24, 2009 and reaches a minimum on mid-day of May 25, 2009. Wind speed in a tropical cyclone is defined as the pressure gradient or difference in pressure between the lowest pressure in the center of the storm and pressure outside the storm (average sea level pressure 1013 mb), divided by the distance over which the pressure change happens. The lower the pressure will fetch to higher wind speed, intense cyclonic activity. Thus a strong negative correlation exists between oceanic surface wind and central pressure. The gradual decrease of OLR starts around May 20, 2009. Further, the OLR reduces to a low value (<160 W/m^2) on May 22, 2009 and continues till May 24, 2009 around 16°N-25°N. At the time of intensification of depression into cyclonic storm (22–24 May 2009), we found a minimum of central pressure and maximum sustained surface wind and lowered OLR value. The right panel of Fig. 3 depicts the latitude –time cross-section of OLR averaged over 80-90°E (top) and temporal variation (10–15 December 2009) of oceanic surface wind and estimated central pressure during the cyclone "WARD" (bottom). A low OLR value (<160 W/m^2) found between 10 and December 12, 2009, covering the latitude region 6- 10°N; simulataneously, the central pressure started to drop on December 10, 2009 and reached low value on December 12, 2009. In opposite relation to central pressure, the sustained surface wind started to increase and reached a maximum of about 44 knots on December 12, 2009 after it descends.

OLR is an indicator of cloud top heights. Low OLR informs the presence of very high and cold clouds at tropical latitudes, which are presumed to be associated with deep convection. From Fig. 3, the

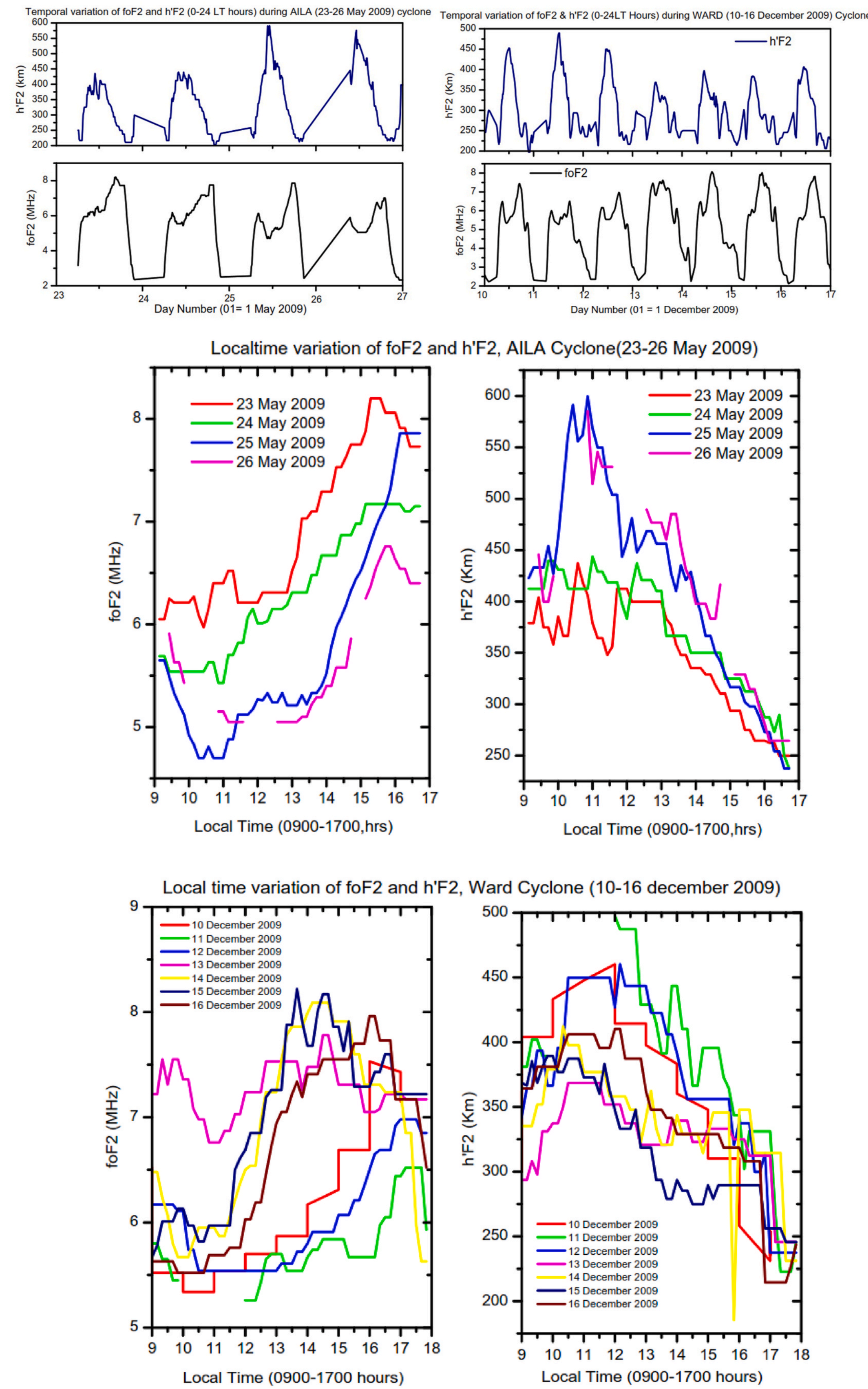

Fig. 2. Temporal variation of foF2 and h'F2 (0–24 LT hours) during the cyclone AILA(left) and WARD (right). a: Local time variation of foF2 and h'F2 (0900–1700 LT hours) during the cyclone AILA(top) and WARD (bottom).

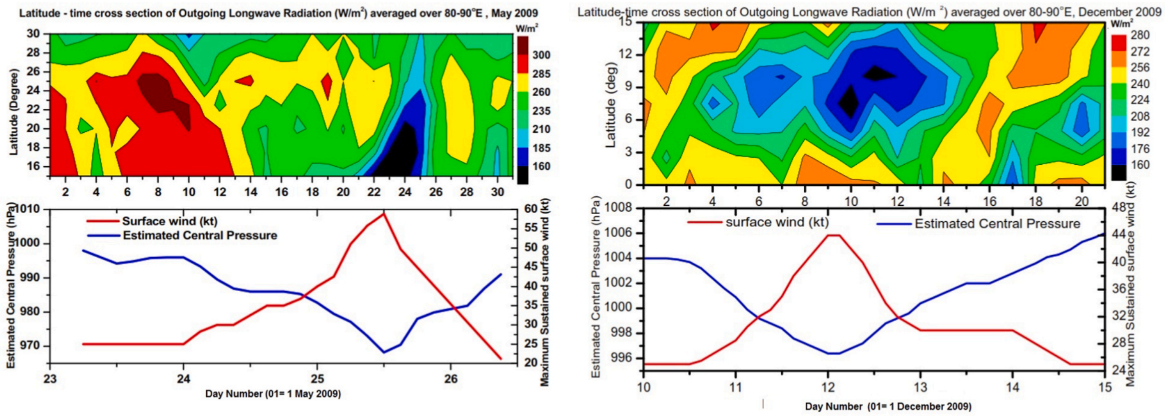

Fig. 3. Temporal variation (23–26 May 2009) of oceanic surface wind and estimated central pressure (bottom) along with latitude time variation of OLR averaged over 80-90°E (top) during the cyclones AILA(left) and WARD (right).

observed low OLR value during the cyclone period informs the presence of deep tropical convection.

3.3. Stratospheric wind variation

Fig. 4 shows the OLR and stratospheric wind conditions during the cyclones AILA (left) and WARD (right). The top left panel of Fig. 4 describes the temporal variation of OLR averaged over latitude 15-30°N and longitude 80-90°N during May 2009. The middle and bottom left panel depicts the zonal and meridional wind conditions during May 2009. From the top left panel, OLR descends and reaches a low value on May 24, 2009. The middle left panel describes the predominance of strong eastward wind at the lower stratosphere in the beginning and middle of May 2009. The vertical profile of zonal wind suggests that a weak eastward wind persists in the lower stratosphere at the time of the entire cyclone period (23–26 May 2009). From the bottom left panel of meridional wind shows the occupancy of weak northward wind in the lower stratosphere during cyclone "AILA."

The top right panel of Fig. 4 describes the temporal variation of OLR averaged over latitude 0-15°N and longitude 80-90°N during December

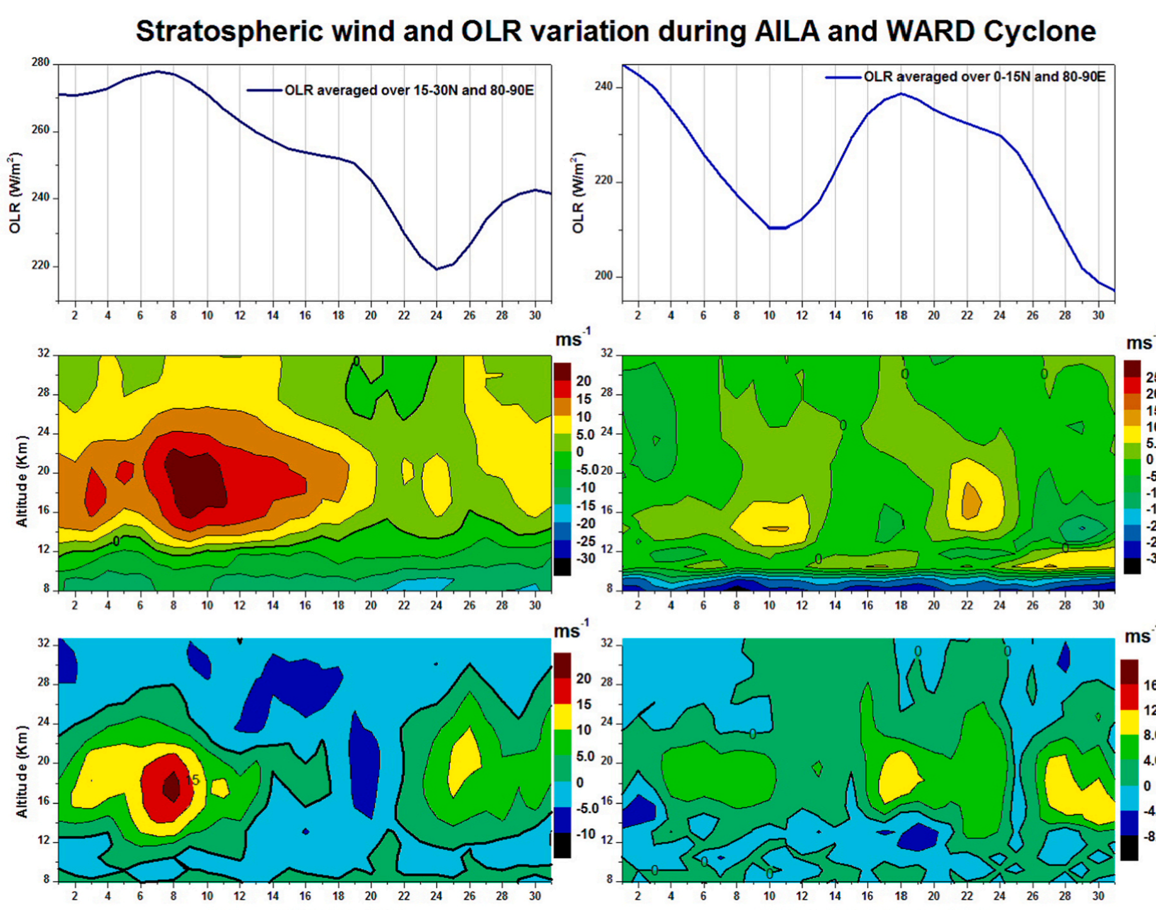

Fig. 4. OLR and stratospheric zonal (middle panel) and meridional wind (bottom panel) conditions during the cyclones AILA (left) and WARD (right). a: Maps of vertical velocities at 200 mb at the time of AILA Cyclone b: Maps of vertical velocities at 200 mb at the time of WARD Cyclone.

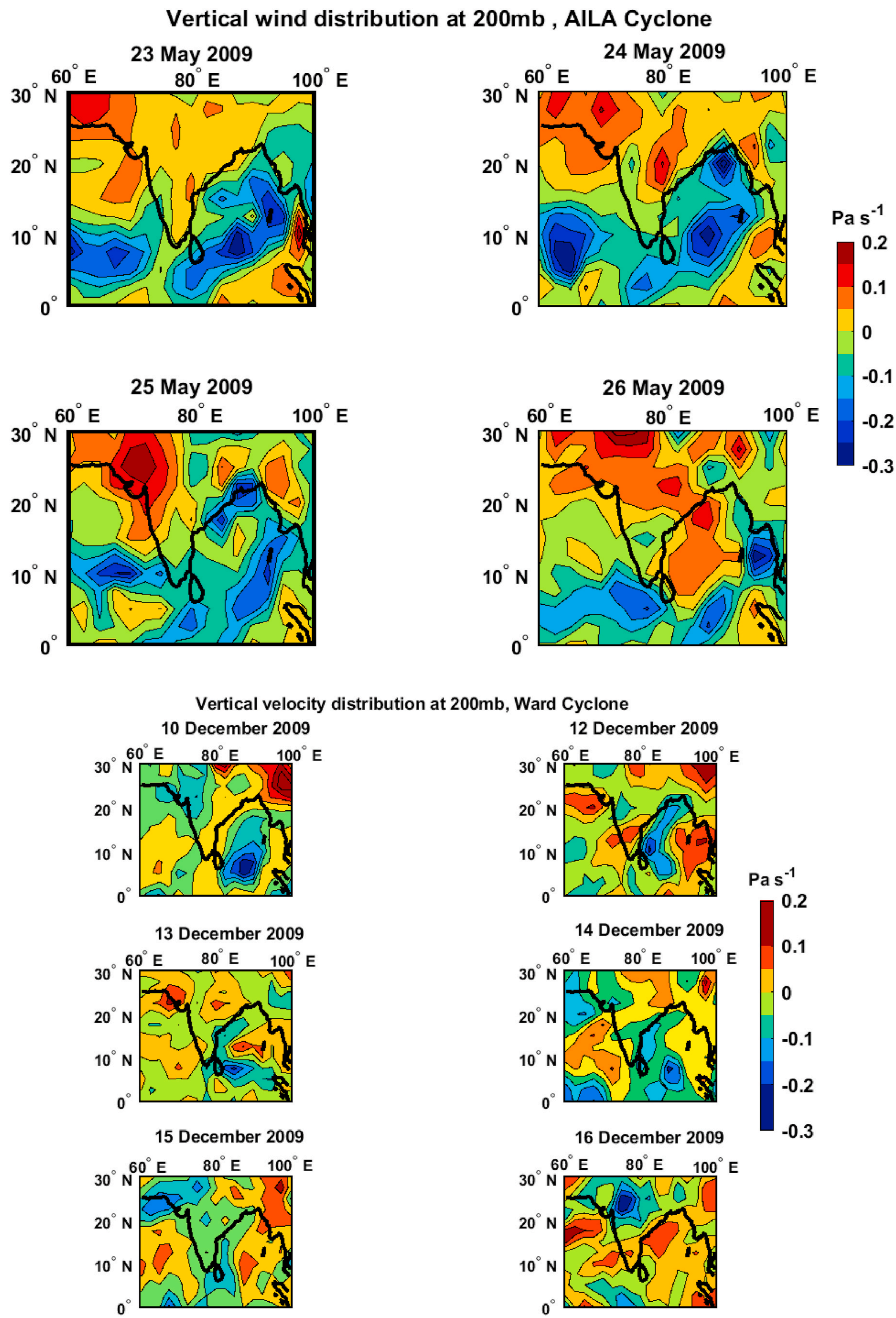

Fig. 4. (*continued*).

2009. The middle and bottom-right panel depicts the zonal and meridional wind conditions during December 2009. From the top right panel, OLR descends and reaches a low value on December 11, 2009. The middle right panel shows the presence of weak eastward wind in the lower stratosphere on December 11, 2009. The zonal wind shows the reversal of eastward to westward transition occurs during the end of the cyclone around December 16, 2009. The meridional wind structure from the bottom right panel also shows the occurrence of weak northward wind in the lower stratosphere at the time of cyclone "WARD."

Fig. 4a depicts the Maps of vertical velocities at 200 mb at the time of AILA Cyclone. It reveals the spatial distribution of vertical wind over the Indian region from 23 to May 26, 2009. Negative values of vertical velocity indicate ascending air, and positive values denote the sinking air. Ascending air motion is associated with cloudiness and rain. The blue color means the upward vertical velocities, and red and yellow indicate the downward velocities. The large upward movement leads to rainfall/convection. From Fig. 4a, we can infer that the extent of upward motion covers the Bay of Bengal region (90°E to 75°E), and the intensity of upward motion maximizes during cyclone days (23 and May 24, 2009) and starts decline on May 25, 2009.

Fig. 4(b) reveals the spatial distribution of vertical velocity at the time of the WARD cyclone. We can see concentrated upward velocities located near Sri Lanka on December 10, 2009. The spread of negative vertical velocity maximizes on 12 and December 13, 2009 at the time of transformation from deep depression into a cyclonic storm. Further, It starts weakening on December 14, 2009 onwards.

Previous research on tropical cyclones reveals that tropical cyclones are an extended and lasting or broadband disturbance source that exists actively for a longer time, and the disturbance propagation covers broadband or zones. The localization of disturbance depends on its propagation direction, either westwards or eastwards, from Tropical cyclone location (L.B. Vanina Dart et al. 2011). We can infer from Fig. 4 (a) and (b), tropical cyclone "AILA" induces broadband convective disturbance covering the Bay of Bengal part, thereby generating low-frequency gravity waves which propagate upward and creates ionospheric disturbance.

3.4. Ionospheric variation during AILA and WARD

Fig. 5 depicts the geomagnetic activities Dst, Kp indices at the time of cyclone events AILA and WARD. The selected cyclone events have quiet geomagnetic conditions, and the influence of geomagnetic activity on the ionospheric layers could be neglected.

The equatorial ionosphere is more sensitive to meteorological events. Fig. 5(a) depicts the local time variation of foF2 and h'F2 at the cyclone events AILA and WARD. The top and bottom left panel reveals the local time variation of h'F2 and foF2 during the cyclone period 23–26 May 2009. The data gaps are labeled in white color. The theory of F2 layer suggests that due to surplus solar ionizing radiation around midday, foF2 maximizes by producing more electrons. On May 25, 2009, at the time of onset of the severe cyclonic storm, increase (decrease) of h'F2 (foF2) extended from ~1000 h to ~1500 LT hours. The maximum increase (decrease) of h'F2 (foF2) occurs before noon time between 1000 and 1200 LT hours. At the time of onset of the severe cyclonic storm, we observed depletion of foF2 and an increase of h'F2. The right panel of Fig. 5(a) depicts the ionospheric foF2 and h'F2 during WARD Cyclone.

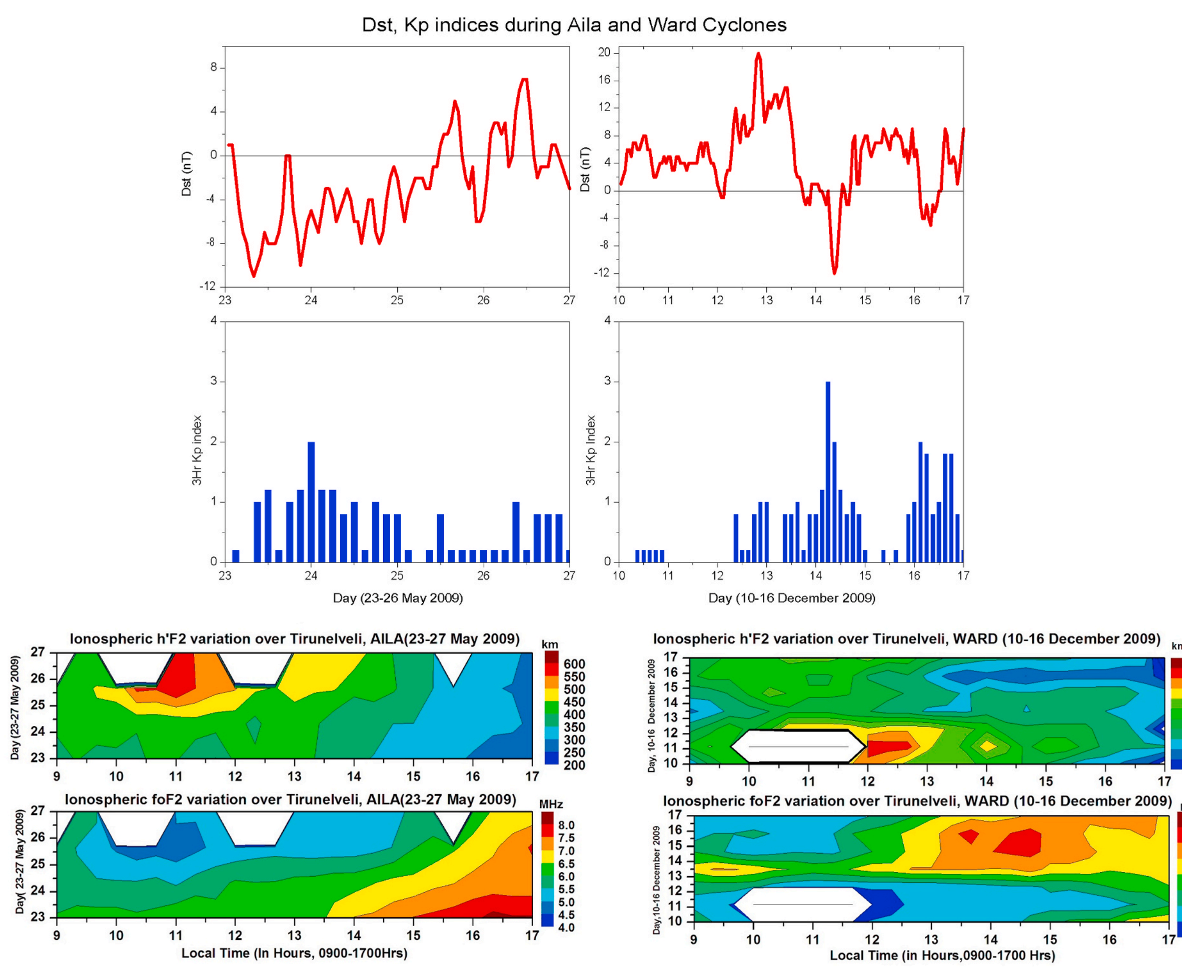

Fig. 5. Temporal variation of Dst, 3-Hr Kp index during AILA and WARD. a: Local time variation of foF2 and h'F2 at the cyclone events AILA (left) and WARD (right).

As we infer from Fig. 5(a), when the cyclone WARD moved to the stages of deep depression and cyclonic storm, between 10 and December 12, 2009, decrement of foF2 found between 0900 and 1600 LT hours and increment of h'F2 found between 1100 and 1300 LT hours. On the recovery phase of WARD cyclone (13–16 December 2009), an enormous increase in foF2 and a decrease in h'F2 found after the noon time (1300–1700 LT hours). From Fig. 5(a), we can infer that at the time of onset of the cyclonic storm stage in AILA and WARD cyclones, the foF2 reduction and h'F2 intensification suggests the prospect of tropical cyclone induced effects on the ionosphere.

3.5. *Gravity wave activity during AILA and WARD cyclone*

Tropical cyclone induced/generated gravity waves propagate upward to the ionosphere and interact with the background flow as Traveling Ionospheric Disturbances (TIDs). Fig. 6 depicts the wavelet spectrum of gravity wave activity during the cyclone AILA and WARD. The hourly wind data from ERA5 Reanalysis has used for finding the gravity wave activity in the stratospheric altitudes at the time of cyclone. Fig. 6 describes the signatures of gravity waves with periods of 2–6 h in foF2, h'F2, and stratospheric wind components. The left panel of Fig. 6 shows the wavelet spectrum of GW activity in foF2, h'F2, zonal (U) and meridional (V) wind at 10 mb (averaged over 80-90°E, 15-30°N) during AILA cyclone. It shows that the dominant presence of GWs of period ~4 h appearing in both stratospheric and ionospheric altitudes between 24 and May 26, 2009. The right panel of Fig. 6 shows the wavelet spectrum of GW activity in foF2, h'F2, zonal (U) and meridional (V) wind at 10 mb (averaged over 80-90°E, 0-15°N). Though some GWs features observed at stratospheric heights (10 mb), the ionospheric foF2 and h'F2 does not show any GW oscillations during cyclone WARD (10–16 December 2009). It suggests that the propagation of GWs might be filtered out by the interaction of background flow at the mesospheric altitudes.

4. Conclusion

The present work is an attempt to describe the equatorial ionospheric response to severe cyclonic storms AILA and WARD observed over the North Indian Ocean. Combined ground observational and reanalysis data are used to reveal the vertical atmosphere – ionosphere coupling mechanism through the tropical cyclone. The different stages of cyclone growth are low pressure, deep depression, cyclonic storm, and severe cyclonic storm etc. At the time of the progress of cyclone intensification from deep depression to cyclonic storm, the oceanic sustained surface wind rises and reaches the maximum. At the same time, significant changes were observed in atmospheric weather; they are, (i) Increased convection (ii) Persistence of weak eastward (northward) wind in zonal (meridional) at stratospheric altitudes (iii) At the onset of cyclonic storm, reduction of foF2 and increase of h'F2 (iv) Propagation of GWs of period ~4hr to Ionospheric heights during AILA. Confirming with our results, Mao et al. (2009) examined the effects of Ionospheric TEC as Typhoon MATSA (1–10 August 2005) passed over Southern China. They found anomalous changes in foF2 and TEC content with the arrival of

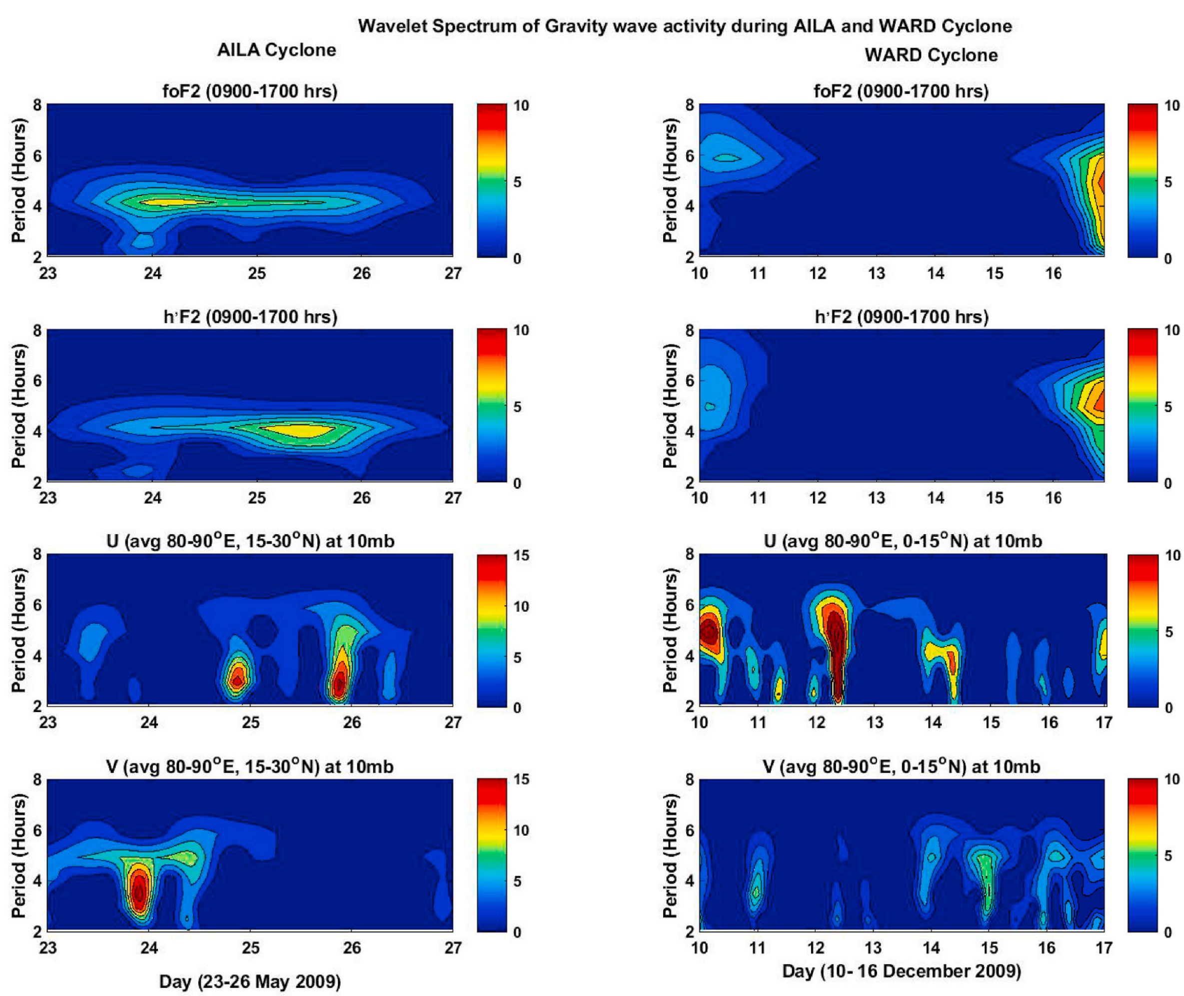

Fig. 6. Wavelet spectrum of gravity wave activity in foF2, h'F2 and Stratospheric zonal wind U (m/s) and meridional wind, V (m/s) at 10 mb during the cyclone AILA (left) and WARD (right).

typhoon because of GW propagate upward and influence the middle and upper atmosphere (Vadas and Fritts, 2004).

The present work describes the tropical cyclone induced ionospheric response by studying two cyclone events AILA and WARD. The two tropical cyclonic storms have behaved distinctly. Earlier researchers found both the conscious possible tropical cyclone – ionosphere connection ((Mikhailov et al., 2005; Vanina-Dart et al., 2007a, 2007b; 2008; Bauer, 1957, 1958; Shen, 1982) and no response in cyclone – ionosphere coupling (Afraimovich et al., 2008).

Afraimovich et al. (2013) investigated ionospheric response to natural and anthropogenic processes using GPS/GLONASS radio soundings during strong TCs Katrina, Rita and Wilma. During Katrina Cyclone, the TEC variations are amplified in the range of periods of 2 to 2 min and of 20–60min. They found the appearance of ionospheric irregularities in the ionosphere above the cyclone trajectory where the radius of the station is about 2000 km from the cyclone centre when it reaches its peak intensity. They observed the ionospheric response to TC Katrina was significantly more robust than the TCs Rita and Wilma. Further, tomographic sounding observations conducted by Vanina-Dart et al., (2011) over three locations at the same meridian Yuzhno-Sakhalinsk (47° N, 143° E), Poronaisk (49° N, 143° E), and Nogliki (51° N, 143° E) suggests the possible influence of a tropical cyclone on the upper ionosphere. They found a significant change in the foF2 parameter by, on average, no more than 10–20% is a possible response of the upper ionosphere localized over the tropical cyclone zone at a distance of approximately 3800–5500 km from it. The tropical cyclone is a wide-band lasting disturbance. A decrease or increase in foF2 is related to the delay of the measurement moment relative to the beginning of the tropical cyclone action. Undoubtedly the mechanism of tropical cyclonic storms influence on the ionosphere is much more complicated because of the collective impact of waves and background. Hence, more case studies to be analyzed, which lead to a comprehensive understanding of the tropical cyclone – ionosphere mechanism.

Declaration of competing interest

The authors declare that they have no known competing financial interests or personal relationships that could have appeared to influence the work reported in this paper.

Acknowledgments

The author thanks all data providing agencies, Cyclone data from the Indian Meteorological Department (IMD), ECMWF ERA-Interim and ERA 5 Reanalysis, Dst Index from World Data Centre of Geomagnetism, Kyoto, and OLR data from National Oceanic and Atmospheric Administration (NOAA) for the present work. The author thankful to the Director, Indian Institute of Geomagnetism Navi Mumbai, for providing Ionosonde data. The author would like to thank the Editor and the two anonymous referees for their critical evaluation of the manuscript.

References

Afraimovich, E.L., Kosogorov, E.A., Leonovich, L.A., Palamartchouk, K.S., Perevalova, N. P., Pirog, O.M., 2000. Determining parameters of large-scale traveling ionospheric disturbances of auroral origin using GPS-arrays. J. Atmos. Sol. Terr. Phys. 62, 553–565. https://doi.org/10.1016/S1364-6826(00)00011-0.

Afraimovich, E.L., Voeykov, S.V., Ishin, A.B., Perevalova, N.P., Ruzhin, YuYa, 2008. Variations in the total electron content during the powerful typhoon of August 5–11, 2006, near the southeastern coast of China. Geomagn. Aeron. 48 (5), 703–708.

Afraimovich, E.L., Gavrilyuk, Nadezhda S., Astafyeva, Elvira I., Demyanov, Vladislav V., Edemskiy, Ilya K., Palamartchouk, Kirill S., Ishin, Artem B., Kosogorov, Eugene A., Leonovich, Lyudmila A., Lesyuta, Oleg S., Voeykov, Sergey V., Perevalova, Natalia P., Polyakova, Anna S., Smolkov, Gennadyi Y., Yasyukevich, Yury V., Zhivetiev, Ilya V., 2013. A review of GPS/GLONASS studies of the ionospheric response to natural and anthropogenic processes and phenomena. J. Space Weather Space Clim. 3, A27. https://doi.org/10.1051/swsc/2013049.

Annual Report, 2009. India Meteorological Department, Complied & Edited by Publication Division, India Meteorological Department,Mausam Bhawan, Lodi Road, New Delhi-110003. https://metnet.imd.gov.in/imdnews/ar2009.pdf.

Altadill, D., Apostolov, E.M., Boska, J., Lastovicka, J., Sauli, P., 2004. Planetary and gravity wave signatures in the F-region ionosphere with impact on radio propagation predictions and variability. Ann. Geophys. 47 (Suppl. 2–3), 1109–1119. https://doi.org/10.4401/ag-3288.

Arendt, P.R., Frisby, E.E.M., 1968. Possible relation of a specific ionospheric event to simultaneous meteorological data. Nature 219, 475–476. https://doi.org/10.1038/219475a0.

Bauer, S.J., 1957. A possible troposphere-ionosphere relationship. J. Geophys. Res. 62, 425–430. https://doi.org/10.1029/JZ062i003p00425.

Bauer, S.J., 1958. An apparent ionospheric response to the passage of hurricanes. J. Geophys. Res. 63, 265–269. https://doi.org/10.1029/JZ063i001p00265.

Bishop, R.L., Straus, P.R., 2006. Characterizing ionospheric variations in the vicinity of hurricanes and typhoons using GPS Occultation Measurements. In: AGU Fall Meeting. San Francisco, 11-15 December. EOS (Trans. Am.Geophys. Union), vol. 87. Suppl.), SA33B-0276.

Boska, J., Sauli, P., 2001. Observations of gravity waves of meteorological origin in theF-region ionosphere. Phys. Chem. Earth C Sol. Terr. Planet Sci. 26 (6), 425–428. https://doi.org/10.1016/S1464-1917(01)00024-1.

Cang, Z., Cheng, G., Cheng, G., 2015. Ionospheric anomalous disturbance during the tropospheric strong convective weather. J. Atmos. Sol. Terr. Phys. 129, 55–61. https://doi.org/10.1016/j.jastp.2015.04.006.

Chen, P.R., 1992. Evidence of the ionospheric response to the QBO. Geophys. Res. Lett. 19, 1089–1092. https://doi.org/10.1029/91GL01564.

Dee, D., Uppala, S., Simmons, A., Berrisford, P., Poli, P., Kobayashi, S., Andreae, U., Balmaseda, M., Balsamo, G., Bauer, P., Bechtold, P., Beljaars, A., Van de Berg, L., Bidlot, J., Bormann, N., Delsol, C., Dragani, R., Fuentes, M., Geer, A., Haimberger, L., Healy, S., Hersbach, H., Hólm, E., Isaksen, L., Kållberg, P., Köhler, M., Matricardi, M., McNally, A., Monge- Sanz, B., Morcrette, J.-J., Park, B.-K., Peubey, C., de Rosnay, P., Tavolato, C., Thépaut, J.-N., Vitart, F., 2011. The ERA Interim reanalysis: configuration and performance of the data assimilation system. Quart. J. Roy. Meteor. Soc.. 137, 553–597. https://doi.org/10.1002/qj.828.

Forbes, J.M., Leveroni, S., 1992. Quasi 16-day oscillation in the ionosphere. Geophys. Res. Lett. 19 (10), 981–984. https://doi.org/10.1029/92GL00399.

Gherzi, E., 1950. Ionosphere and weather. Nature 165, 38. https://doi.org/10.1038/165038a0.

Goldberg, R.A., 1991. External and internal influences on the global electric circuit. In: Note Presented at the Conference on Major Scientific Problems of the Atmospheric System and the Developing Countries. I.C.T.P., Trieste, Italy, November.

Guha, A., Paul, B., Chakraborty, M., De, B.K., 2016. Tropical cyclone effects on the equatorial ionosphere: first result from the Indian sector. J. Geophys. Res. Space Physics 121, 5764–5777. https://doi.org/10.1002/2016JA022363.

Hendon, H., Woodberry, K., 1993. The diurnal cycle of tropical convection. J. Geophys. Res. 98, 16623–16637. https://doi.org/10.1029/93JD00525.

Hung, R.J., Kuo, J.P., 1978. Ionospheric observation of gravity waves associated with Hurricane Eloise. J. Geophys. 45, 67–80. https://journal.geophysicsjournal.com/JofG/article/view/173.

Kazimirovsky, E., 2002. Coupling from below as a source of ionospheric variability: a review. Ann. Geophys. 45 (1) https://doi.org/10.4401/ag-3482.

Kersley, L., Rees, P.R., 1982. Tropospheric gravity waves and their possible association with medium-scale travelling ionospheric disturbances. J. Atmos. Terr. Phys. 44, 147–159. https://doi.org/10.1016/0021-9169(82)90117-9.

Knížová, K.P., Mošna, Z., Kouba, D., Potužníková, K., Boška, J., 2015. Influence of meteorological systems on the ionosphere over Europe. J. Atmos. Sol. Terr. Phys. 136, 244–250. https://doi.org/10.1016/j.jastp.2015.07.017.

Lastovicka, J., Sauli, P., 1999. Are planetary wave type oscillations in the F2 region caused by planetary wave modulation of upward propagating tides? Adv. Space Res. 24, 1473–1476. https://doi.org/10.1016/S0273-1177(99)00708-5.

Lastovicka, J., 2006. Forcing of the ionosphere by waves from below. J. Atmos. Sol. Terr. Phys. 68, 479–497. https://doi.org/10.1016/j.jastp.2005.01.018.

Liebmann, B., Smith, C.A., 1996. Description of a complete (interpolated) outgoing Longwave radiation dataset. Bull. Am. Meteorol. Soc. 77, 1275–1277. https://www.jstor.org/stable/26233278.

Lin, J.W., 2012. Study of ionospheric anomalies due to impact of typhoon using Principal Component Analysis and image processing. J. Earth Syst. Sci.. 121 (4), 1001–1010. https://doi.org/10.1007/s12040-012-0214-6.

Liu, J.Y., Tsai, H.F., Lin, C.H., Kamogawa, M., Chen, Y.I., Lin, C.H., Huang, B.S., Yu, S.B., Yeh, Y.H., 2010. Co-seismic ionospheric disturbances triggered by the Chi–Chi earthquake. J. Geophys. Res. 115, A08303. https://doi.org/10.1029/2009JA014943.

Mao, T., Wang, J.S., Yang, G.L., Yu, T., Ping, J.S., Suo, Y.C., 2009. Effects of typhoon Matsa on ionospheric TEC. Chin. Sci. Bull. 55 (8), 712–717. https://doi.org/10.1007/s11434-009-0472-0.

Manzano, J.R., Radicella, S.M., Zossi de Artigas, M.M., Filippi de Manzano, A.N., Cosio de Ragone, A.H., 1998. Troposphere-ionosphere interaction during tropospheric mesoscale convective complexes events. J. Atmos. Sol. Terr. Phys. 60 (6), 585–594. https://doi.org/10.1016/S1364-6826(98)00002-9.

Mikhailov, YuM., Mikhailova, G.A., Kapustina, O.V., Druzhin, G.I., Cherneva, N.V., 2005. Possible atmospheric effects in the lower ionosphere according to atmospheric radio noise observations on kamchatka during tropical cyclones. Geomagn. Aeron. 45 (6), 824–839.

Pancheva, D., Alberca, L.F., de la Morena, B.A., 1994. Simultaneous observation of the quasi-two day variations in the lower and upper ionosphere. J. Atmos. Sol. Terr. Phys. 56, 43–50. https://doi.org/10.1016/0021-9169(94)90174-0.

Perevalova, Nataly P., Polekh, Nelya M., 2009. An investigation of the upper atmosphere response to cyclones using ionosonde data in Eastern Siberia and the Far East. In:

Proc. SPIE 7296, Fifteenth International Symposium on Atmospheric and Ocean Optics/Atmospheric Physics, p. 72960J. https://doi.org/10.1117/12.823814.

Polyakova, A.S., Perevalova, N.P., 2011. Investigation into impact of tropical cyclones on the ionosphere using GPS sounding and NCEP/NCAR Reanalysis data. Adv. Space Res. 48, 1196–1210. https://doi.org/10.1016/j.asr.2011.06.014.

Polyakova, A.S., Perevalova, N.P., 2013. Comparative analysis of total electron content disturbances over nine tropical cyclones. Sovremennye problemy distantsionnogo zondirovaniya Zemli iz kosmosa 10 (2), 197–205.

Pulinets, S.A., Legen'ka, A.D., Gaivoronskaya, T.V., Depuev, V. Kh, 2003. Main phenomenological features of ionospheric precursors of strong earthquakes. J. Atmos. Sol. Terr. Phys. 65 (16), 1337–1347. https://doi.org/10.1016/j.jastp.2003.07.011.

Radicella, S.M., Sauli, P., Jakowski, N., Kouba, D., Portillo, A., Herraiz, M., Strangeways, H.J., Zernov, N., Gherm, V., 2009. Space plasma effects. Ann. Geophys. 52 (3–4), 359–372. https://doi.org/10.4401/ag-4583.

Roy, C., Kovordanyi, R., 2018. In: Bartlett, D., Singh, R. (Eds.), Tropical Cyclone and Track Forecasting. Exploring Natural Hazards: A Case Study Approach. Chapman and Hall/CRC, New York, pp. 1–48. https://doi.org/10.1201/9781315166858.

Shen, C.S., 1982. The correlations between the typhoon and the foF2 of ionosphere. Chin. J. Space Sci. 2 (4), 335–340.

Shresta, K.L., 1971a. A Sporadic-E and atmospheric pressure waves. J. Atmos. Terr. Phys. 33, 205–211. https://doi.org/10.1016/0021-9169(71)90196-6.

Shresta, K.L., 1971b. Anomalous ionospheric absorption and micro barometric activity at ground level. J. Atmos. Terr. Phys. 33, 213–219. https://doi.org/10.1016/0021-9169(71)90197-8.

Sindelarova, Tereza, buresova, dalia, chum, Jaroslav, 2009. Observations of acoustic gravity waves in the ionosphere generated by severe tropospheric weather. Studia Geophys. Geod. 53, 403–418. https://doi.org/10.1007/s11200-009-0028-4.

Sun, L., Wan, W., Ding, F., Mao, T., 2007. Gravity wave propagation in the realistic atmosphere based on a three-dimensional transfer function model. Ann. Geophys. 25, 1979–1986. https://doi.org/10.5194/angeo-25-1979-2007.

Vadas, S.L., Fritts, 2004. Thermospheric responses to gravity waves arising from mesoscale convective complexes. J. Atmos. Sol. Terr. Phys. 66, 781–804. https://doi.org/10.1016/j.jastp.2004.01.025.

Vanina-Dart, L.B., Romanov, A.A., Sharkov, E.A., 2011. Influence of a tropical cyclone on the upper ionosphere according to tomography sounding data over sakhalin island in november 2007. Geomagn. Aeron. 51 (No. 6), 774–782. https://doi.org/10.1134/S001679321106017X. ISSN 0016–7932.

Vanina-Dart, L.B., Pokrovskaya, I.V., Sharkov, E.A., 2007a. Studying the interaction between the lower equatorial ionosphere and tropical cyclones according to data of remote and rocket sounding. Issled. Zemli Kosm 2, 19–27.

Vanina-Dart, L.B., Pokrovskaya, I.V., Sharkov, E.A., 2007b. Effect of solar activity on the response of the lower equatorial ionosphere during the active phase of tropical cyclones. Issled. Zemli Kosm.. 6, 3–10.

Vanina-Dart, L.B., Pokrovskaya, I.V., Sharkov, E.A., 2008. Response of the lower equatorial ionosphere to strong tropospheric disturbances. Geomagn. Aeron. 48 (2), 255–260.

Xu, G., Wan, W., She, C., Du, L., 2008. The relationship between ionospheric total electron content (TEC) over East Asia and the tropospheric circulation around the Qinghai-Tibet Plateau obtained with a partial correlation method. Adv. Space Res. 42 (1), 219–223. https://doi.org/10.1016/j.asr.2008.01.007.

Yi, Luo, Chen, P.R., 1993. Long period oscillations in the equatorial ionization anomaly correlated with the neutral wind in the mesosphere. J. Atmos. Terr. Phys. 55, 1317–1323. https://doi.org/10.1016/0021-9169(93)90100-D.